

7 Strong undulators

7.1 The trajectory in the strong undulator

Let us return to the equation of motion of the electron in the harmonic undulator field, i.e.

$$\ddot{x} = -\frac{eB_0}{m\gamma} \cos(k_u z) \dot{z}, \quad \ddot{z} = \frac{eB_0}{m\gamma} \cos(k_u z) \dot{x},$$

with integration of the first equation to

$$\dot{x} = -\frac{cK_u}{\gamma} \sin(k_u z)$$

and because of the conservation of energy

$$\dot{z} = \beta c \sqrt{1 - \frac{K_u^2}{\beta^2 \gamma^2} \sin^2(k_u z)}.$$

For the weak undulator, we assumed that the average drift velocity of the particle in the z direction is equal to the instantaneous velocity βc , and in this approximation we obtained a simple sinusoidal trajectory for the particle.

We now abandon this approximation.

Without this approximation, the trajectory angle as a function of z is obtained as follows

$$x' = \frac{dx}{dz} = \frac{\dot{x}}{\dot{z}} = -\frac{K_u \sin(k_u z)}{\beta \gamma \sqrt{1 - \frac{K_u^2}{\beta^2 \gamma^2} \sin^2(k_u z)}}. \quad (7.1)$$

From this, the trajectory can in principle be calculated, but the solution leads to an elliptic integral. However, on closer inspection, it can be seen that under the condition for the extrema of x' (which is still valid in the ultrarelativistic case of interest here)

$$\hat{x}' = \tan \psi_0 \ll 1 \quad \Rightarrow \quad \hat{x}' \approx \psi_0 \approx \frac{K_u}{\beta \gamma} \ll 1 \quad (7.2)$$

as well as the approximation for observation from a large distance

$$\frac{L_u}{r_p} \ll 1 \quad (7.3)$$

our approximation above for the trajectory

$$x'(z) = -\frac{K_u}{\beta \gamma} \sin(k_u z), \quad x(z) = \frac{K_u}{k_u \beta \gamma} \cos(k_u z) \quad (7.4)$$

remains justified and can be approximated for motion in the z direction

$$\begin{aligned} \frac{dz}{dt'} &\approx \beta c \left(1 - \frac{K_u^2}{2\beta^2\gamma^2} \sin^2(k_u z) \right) \\ \Leftrightarrow \beta c dt' &= \frac{dz}{\left(1 - \frac{K_u^2}{2\beta^2\gamma^2} \sin^2(k_u z) \right)} \end{aligned} \quad (7.5)$$

Here we have developed the root to the second member.

In our equation, \dot{z} is a function of z . To get to $z(t')$ or $\dot{z}(t')$, we first have to integrate:

$$\beta c \int_0^{t'} dt'' = \int_0^{z(t')} \frac{1}{1 - \frac{K_u^2}{2\beta^2\gamma^2} \sin^2(k_u z')} dz' \quad (7.6)$$

and differentiate again with respect to t' for $\dot{z}(t')$. If we do this and also express the x component of the trajectory as a function of the emission time t' , we obtain the equations of motion

$$\begin{aligned} \dot{x}(t') &= -\frac{cK_u}{\gamma} \sin(\Omega_u t'), & \dot{z}(t') &= \beta^* c + \frac{cK_u^2}{4\beta^2\gamma^2} \cos(2\Omega_u t') \\ x(t') &= \frac{K_u}{\beta\gamma k_u} \cos(\Omega_u t'), & z(t') &= \beta^* c t' + \frac{K_u^2}{8\beta^2\gamma^2 k_u} \sin(2\Omega_u t'). \end{aligned} \quad (7.7)$$

The motion in the z -direction now consists of a uniform drift with the average drift velocity

$$\beta^* c = \beta c \left(1 - \frac{K_u^2}{4\beta^2\gamma^2} \right) < \beta c \quad (7.8)$$

with an oscillatory modulation with the frequency and amplitude

$$2\Omega_u = 2k_u \beta^* c, \quad \hat{z} = \frac{K_u^2}{4\beta^2\gamma^2} \beta c \quad (7.9)$$

According to the reduced mean speed, the Lorentz factor is also reduced:

$$\gamma^* = \frac{1}{\sqrt{1 - \beta^{*2}}} \approx \frac{\gamma}{\sqrt{1 + \frac{K_u^2}{2}}} < \gamma. \quad (7.10)$$

For illustration purposes, we will show the particle motion in the system that is moved along with $\beta^* c$. The LORENTZ transformation into this system leads to the aforementioned 8-shaped motion with oscillation components in both the x and z directions:

$$x^*(t) = \frac{K_u^*}{\beta\gamma^* k_u} \cos(\Omega_u^* t), \quad z^*(t) = \frac{(K_u^*)^2}{8\beta^2\gamma^* k_u} \sin(2\Omega_u^* t) \quad (7.11)$$

with

$$\Omega_u^* = \gamma^* k_u \beta^* c \quad (7.12)$$

and the modified undulator parameter

$$K_u^* := \frac{K_u}{\sqrt{1 + \frac{K_u^2}{2}}} \approx \psi_0 \gamma^*. \quad (7.13)$$

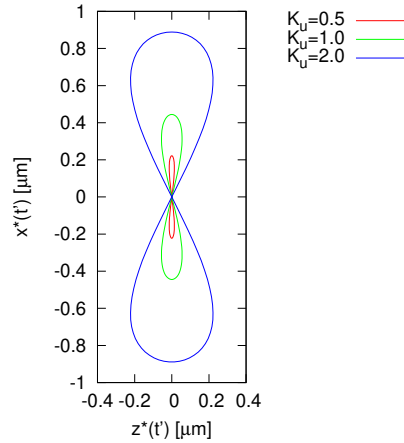


Figure 29: Trajectory of the particle in the co-moving inertial system K^* . The calculation was based on the parameters of SCU14 at ANKA: $\lambda_u = 14$ mm, $\gamma = 4900$.

Now the terms of the distance vector between particle and observer, the velocity and the acceleration that go into the calculation of the radiation field can be set up again:

7.2 The radiation of the strong undulator

The radiation field of the strong undulator can be calculated in a similar way to that for the weak undulator or normal synchrotron radiation from the trajectory of the particle and the relation of the time scales, which are completely contained in the established equations of motion. Explicitly, these are

$$\begin{aligned} \vec{r}(t') &= \begin{pmatrix} \frac{K_u}{\beta \gamma k_u} \cos \Omega_u t' \\ 0 \\ \beta^* c t' + \frac{K_u^2}{8 \beta^2 \gamma^2 k_u} \sin 2 \Omega_u t' \end{pmatrix} \\ \vec{\beta}(t') &= \begin{pmatrix} -\frac{K_u}{\gamma} \sin \Omega_u t' \\ 0 \\ \beta^* + \frac{K_u^2}{4 \beta \gamma^2} \cos 2 \Omega_u t' \end{pmatrix} \\ \dot{\vec{\beta}}(t') &= \begin{pmatrix} -\frac{\beta c k_u K_u}{\cos} \Omega_u t' \\ 0 \\ -\frac{K_u^2 k_u c}{2 \gamma^2} \sin 2 \Omega_u t' \end{pmatrix}. \end{aligned} \quad (7.14)$$

With

$$\vec{R} = \vec{r}_p - \vec{r}$$

and the retardation condition, the following results for the relation of the time scales (formulated for the reduced observer time):

$$\begin{aligned} t_p &= t' + \frac{R(t') - r_p}{c} \\ &= \frac{1}{\omega_1} (\Omega_u t' - b_u \cos \Omega_u t' - a_u \sin 2\Omega_u t') \end{aligned} \quad (7.15)$$

with

$$\omega_1 = \frac{2\gamma^{*2}\Omega_u}{1 + \gamma^{*2}\vartheta^2} \quad (7.16)$$

the fundamental frequency of the radiation field as a function of the viewing angle ϑ and the amplitudes of the oscillatory terms

$$a_u = \frac{K_u^{*2}}{4(1 + \gamma^{*2}\vartheta^2)}, \quad b_u = \frac{2K_u^*\gamma^*\vartheta \cos \varphi}{1 + \gamma^{*2}\vartheta^2}. \quad (7.17)$$

The first crucial finding is already contained in equation 7.16: Reducing the average drift velocity \bar{v} leads to a reduction in the fundamental frequency. Transforming equation 7.16 according to the original characteristic quantities for electron energy and undulator results in the *undulator equation*

$$\omega_1 = \frac{4\pi c\gamma^2}{\lambda_u(1 + \frac{K_u^2}{2} + \gamma^2\vartheta^2)} \quad \Leftrightarrow \quad \lambda_1 = \frac{\lambda_u}{2\gamma^2} \left(1 + \frac{K_u^2}{2} + \gamma^2\vartheta^2 \right) \quad (7.18)$$

The substitution of the equation of motion into the radiation term is analogous to the previously treated cases of normal synchrotron radiation and weak undulators and will not be explicitly repeated here. The crucial difference to the previously treated cases is that we are now dealing with a complex periodic motion, i.e. the radiation field is periodic but cannot be described by a pure sine. The 'transition to the frequency domain in this case is therefore done via a Fourier series expansion:

$$\vec{E}(t_p) = \sum_{h=-\infty}^{\infty} \vec{E}_h e^{ih\omega_1 t_p} \quad \text{with} \quad \vec{E}_h = \frac{1}{T_p} \int_0^{T_p} \vec{E}(t_p) e^{-ih\omega_1 t_p} dt_p \quad (7.19)$$

where $T_p = \frac{2\pi}{\omega_1}$ is the period of the radiation field.

Our radiation field is now represented by a series of harmonic Fourier components at the K_u - and ϑ -dependent fundamental frequency ω_1 .

We will not go into the Fourier integrals after substituting the equations of motion into the series expansion of the radiation field here (those interested are referred to A. Hofmann, *The Physics of Synchrotron Radiation*).

We now move directly on to the resulting spectral and angular distribution of the radiation power. This is obtained as the sum of the contributions for the harmonics

$$\boxed{\frac{d^2 P_h}{d\Omega d\omega} = P_u \gamma^{*2} [F_{h\sigma}(\vartheta, \varphi) + F_{h\pi}(\vartheta, \varphi)] f_N(\Delta\omega_h)} \quad (7.20)$$

with the total radiant power

$$P_u = \frac{2r_0 c^3 e^2 \langle B^2 \rangle W_e^2}{3(mc^2)^3} \quad (7.21)$$

as in the case of the weak undulator, the angular distribution functions

$$\begin{aligned} F_{h\sigma}(\vartheta, \varphi) &= \frac{3h^2}{\pi(1 + K_u^2/2)K_u^{*2}} \frac{(2\Sigma_{h1}\gamma^*\vartheta \cos\varphi - \Sigma_{h2}K_u^*)^2}{(1 + \gamma^{*2}\vartheta^2)^3} \\ F_{h\pi}(\vartheta, \varphi) &= \frac{3h^2}{\pi(1 + K_u^2/2)K_u^{*2}} \frac{(2\Sigma_{h1}\gamma^*\vartheta \sin\varphi)^2}{(1 + \gamma^{*2}\vartheta^2)^3}, \end{aligned} \quad (7.22)$$

which are the series 'via the Bessel functions

$$\begin{aligned} \Sigma_{h1} &:= \sum_{l=-\infty}^{\infty} J_l(ha_u) J_{h+2l}(hb_u) \\ \Sigma_{h2} &:= \sum_{l=-\infty}^{\infty} J_l(ha_u) J_{h+2l+1}(hb_u) + J_l(ha_u) J_{h+2l-1}(hb_u), \end{aligned} \quad (7.23)$$

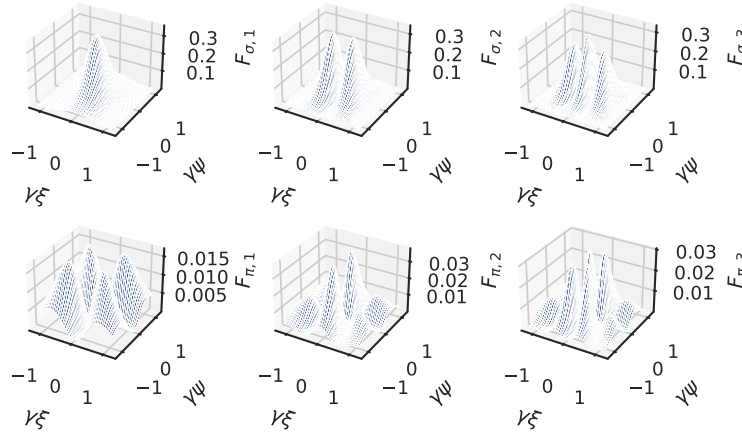
The spectral functions are analogous to the weak undulator

$$f_N(\Delta\omega_h) = \frac{N_u}{\omega_1} \left(\frac{\sin\left(\frac{\Delta\omega_h}{\omega_1} \pi N_u\right)}{\frac{\Delta\omega_h}{\omega_1} \pi N_u} \right)^2 \quad (7.24)$$

with

$$\omega_h = h\omega_1, \quad \frac{\Delta\omega_h}{\omega_1} = \frac{\omega - h\omega_1}{\omega_1} \quad (7.25)$$

The following tables show the spectrally integrated angular distribution functions and the angle-integrated spectra of the first three harmonics of the radiation from the strong undulator. As with the weak undulator, the angle dependence of the observed frequency leads to Doppler-broadened spectral distributions with the respective cutoff frequency ω_h . The spectra shown are those of an infinitely long strong undulator.

Angular distribution of the radiation power

The following applies to the angular distributions:

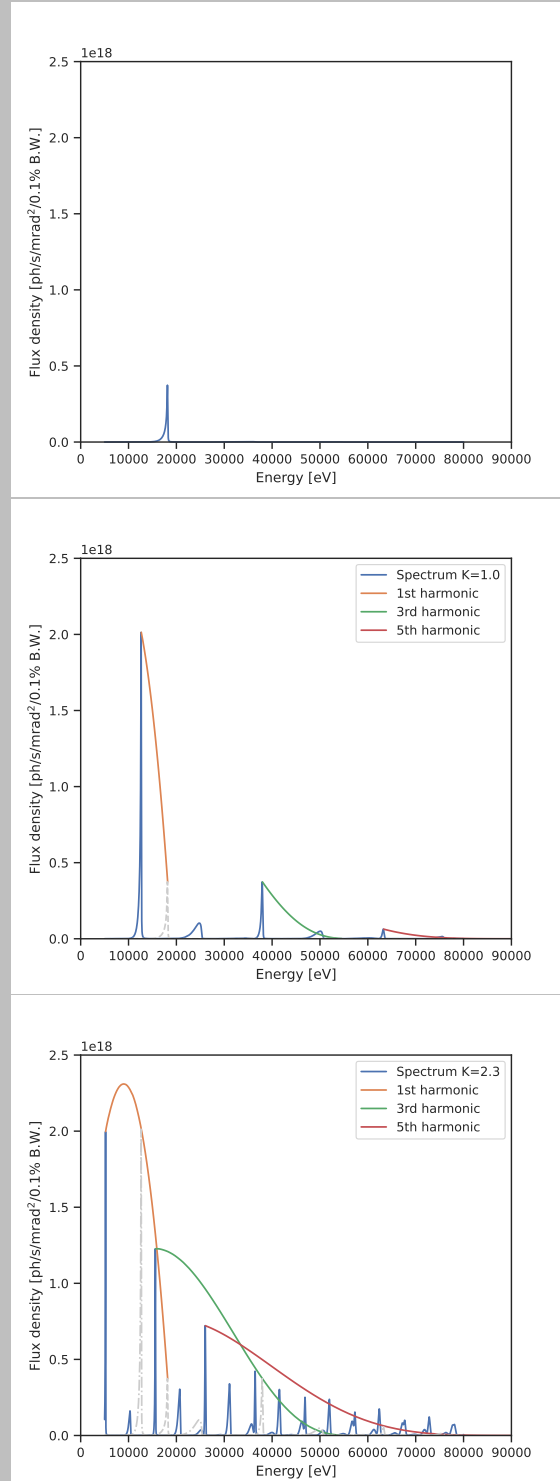
- Odd harmonic, σ polarisation: maximum on the undulator axis, $h - 1$ node lines perpendicular to the x axis
- Odd harmonic, π polarisation: node lines at $x = 0, y = 0$ and $h - 1$ node lines perpendicular to the x axis
- even harmonic, σ polarisation: nodal line at $x = 0$, $h - 2$ nodal lines perpendicular to the x -axis
- even harmonic, π polarisation: nodal line at $y = 0$ and h nodal lines perpendicular to the x -axis

As in the case of the weak undulator, the spectral-angular photon flux density (which is particularly important for the application) can be specified for the strong undulator for each harmonic on the beam axis ($\vartheta = 0$) and at the respective central frequency $\omega = \omega_{h0} = h\omega_{10}$ at an electron current I . This results in:

$$\frac{d^2 \dot{n}_{hI}}{d\Omega d\omega/\omega_h} = \frac{\alpha_f h^3 \gamma^2 I K_u^2 N_u^2}{e(1 + K_u^2/2)^2} \left[J_{(h-1)/2} \left(h \frac{K_u^{*2}}{4} \right) - J_{(h+1)/2} \left(h \frac{K_u^{*2}}{4} \right) \right]^2 \quad (7.26)$$

This expression can now be used to calculate the undulator *tuning curves*, i.e. the plot of the flux 'over the photon energy, which for a given γ , λ_u and K_u results from the undulator equation 7.18.

Undulator spectra and tuning



- the undulator spectrum can be changed by varying $K_u = \frac{e}{2\pi mc} B_0 \lambda_u$
- $K_u = 0.3$: virtually harmonic motion \rightarrow single line spectrum
- $K_u = 1.0$: higher harmonics appear, intensity increases (power $\propto B_0^2$), lines are shifted to longer wavelengths (lower energies)
- $K_u = 2.3$: tuning ranges of 1st and 3rd harmonic overlap

Finally, let us look at some examples:

Undulator Tuning Curves: Examples

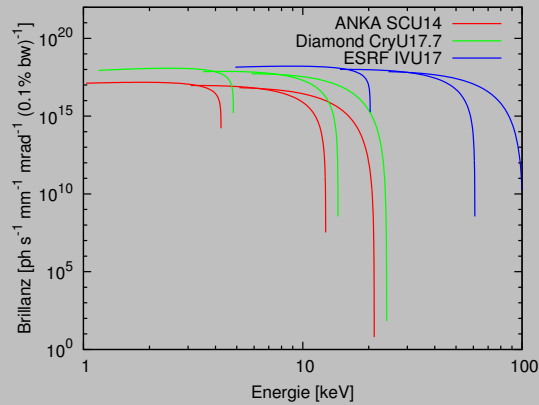


Figure 30: Tuning curves of undulators: ANKA superconducting undulator, Diamond cooled undulator, ESRF in-vacuum undulator

Undulator spectra for $K=2$

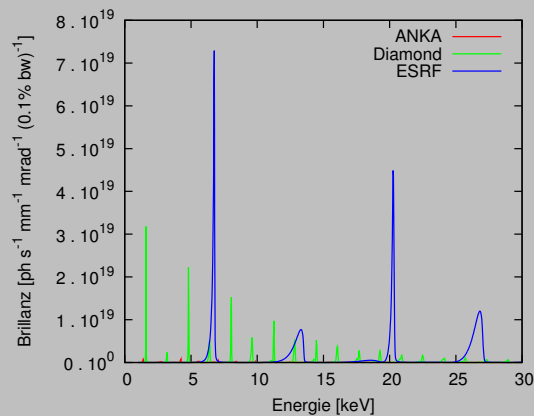


Figure 31: Undulator spectra for $K_u = 2$ in linear representation for the same sources

Remark. The wiggler can be treated as a very strong undulator with K_u so large and N_u so small that the spacing of the harmonics becomes smaller than the width of the spectral function. Result: quasicontinuous spectrum.

References

Hofmann, Albert (2004). *The Physics of Synchrotron Radiation*. Cambridge Monographs on Particle Physics, Nuclear Physics and Cosmology. Cambridge: Cambridge University Press. ISBN: 978-0-521-30826-7. DOI: [10.1017/CB09780511534973](https://doi.org/10.1017/CB09780511534973).